



2D-NANOLATTICES

FP7-ICT-2009-C (FET Open)

***Highly anisotropic graphite-like semiconductor/dielectric
2D nanolattices***

Deliverable D3.1

In situ STM identification of the honeycomb structure of 2D-nanolattices of silicene and germanene

Report

Prepared by Prof G. Le Lay, Aix-Marseille University

Contributors: CNRS, NCSR-D, CNR

Preparation Date: 15/06/2012

Report version number: final

Classification: Public

Contract Start Date: 01/06/2011

Duration: 36 months

Project Coordinator: NCSR- D (*Dr. A. Dimoulas*)

Contractors: IMEC, KULeuven, CNR, CNRS, U. de Provence

**Project funded by the European Community under the
“Future and Emerging Technologies” Programme**

Table of contents

Introduction	page 3
Present status	3
CNRS-/Aix-Marseille U. contribution	3
NCSR-D contribution	6
CNR-IMM contribution	14
Conclusion	21

Introduction

It is one of the main initial aim of the 2D-Nanolattices “Highly anisotropic graphite-like semiconductors/dielectric 2D nanolattices” project to demonstrate the synthesis of silicene and germanene, the graphene analogues for silicon and germanium, which, at variance with graphene, do not exist in nature. This is, indeed, a real challenge!

In the following we will present preparation, growth and characterization of atom-thin 2D silicon and germanium films on Ag(111) and other single crystal (111) metal surfaces. Success in the silicene synthesis has been achieved (two publications, one already published, one in press), while encouraging results have been obtained toward the aim of synthesizing also germanene.

Present status

Contractor: CNRS-CINaM, (9 person months)

Milestone 1: Prove the existence of Silicene and Germanene on metal substrates.

Silicene: our contribution to the state of the art

The first multi techniques experimental article on silicene has been accepted for publication at the beginning of March 2012 [1]. Therein is contained a detailed description of experimental evidences of the silicene existence, evidences obtained from 4 combined techniques: STM, LEED, ARPES, and DFT. STM and LEED provided structural information and some basic electronic information. ARPES was the key tool to prove the silicene existence and justify further investment on the subject. The structural analysis indicates the hexagonal symmetry of the silicon film and a silicon-silicon distance of 0.22 nm. ARPES data proves the presence of linear band dispersion in a cone like shape; from the measured section of the Dirac cone it was possible to calculate a Fermi velocity for electrons in the same order of magnitude of graphene $1.3 \times 10^6 \text{ ms}^{-1}$. ARPES also confirmed the lattice parameter obtained from STM and LEED. DFT calculations rounds up the publication by supporting the model and confirming the silicene thermodynamically stable on silver.

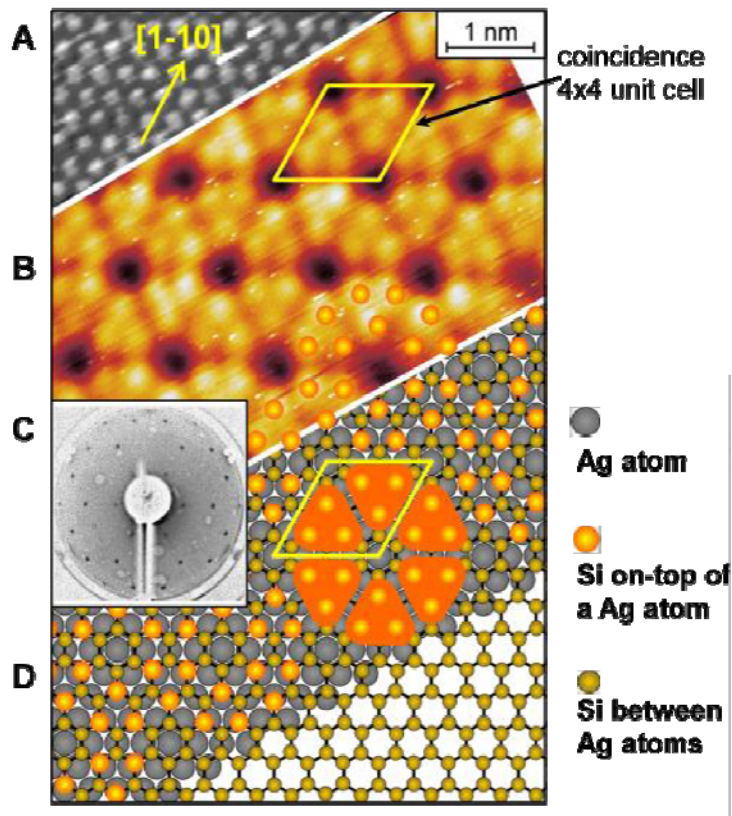


Figure 1: Published model for the 4x4 structure. A) Bare silver, B) 4x4 STM data, C) LEED, D) Ball model of the structure.

Nevertheless the phase diagram for silicon on silver is rather complex and exhibits several structures depending on temperature and surface coverage. So far only the so called 4x4 has been fully characterized and recognized as silicene, nevertheless few of the remaining phases still need further spectroscopic characterization.

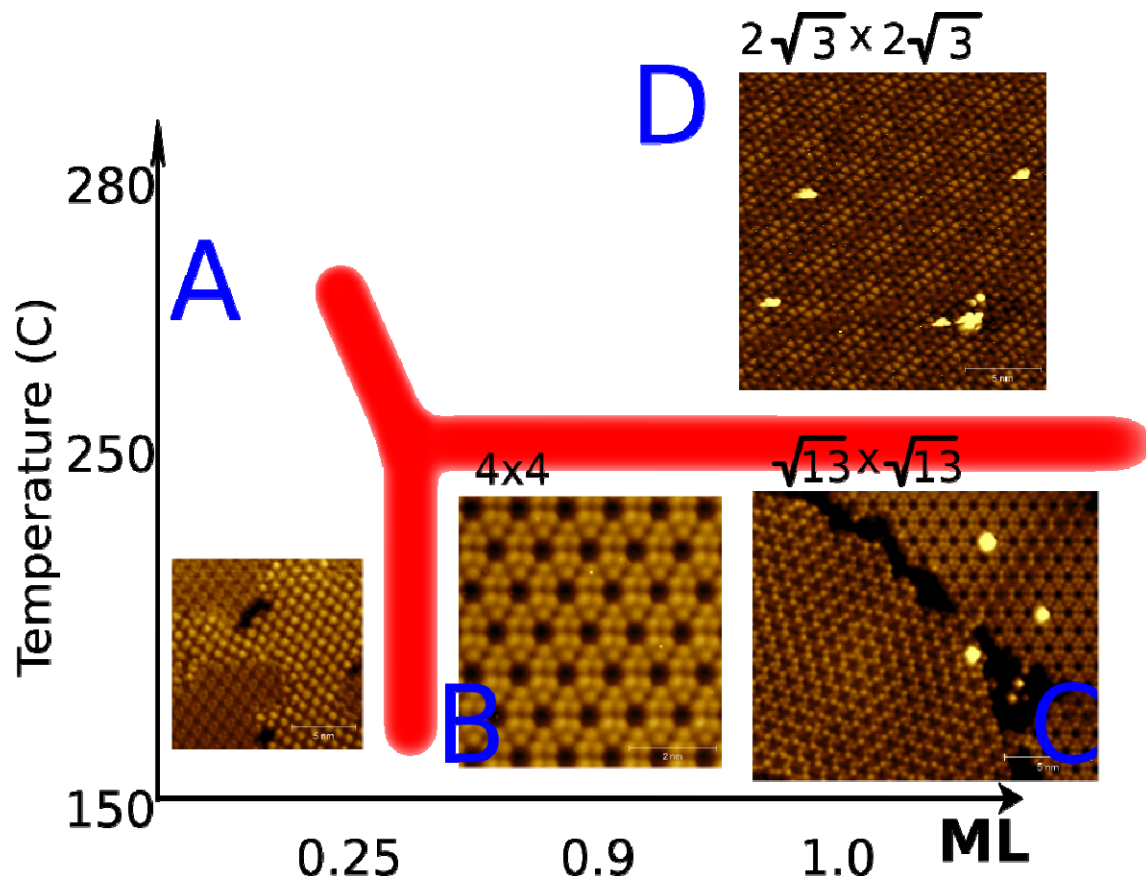


Figure 2: Silicon on Silver phase diagram. A) Low coverage structure, low density protrusions are arranged in hexagonal pattern in a 4x4 manner. B,C) Two structures always co-exist for this range of temperature with a preference for the 4x4 at low temperature, nevertheless the $\sqrt{13} \times \sqrt{13}$ is always present at least as minor component. D) High temperature phase, it appears over 250C.

Publication

Silicene: Compelling experimental evidence for graphene-like two-dimensional silicon

Patrick Vogt, Paola De Padova, Claudio Quaresima, Jose Avila, Emmanouil Frantzeskakis, Maria Carmen Asensio, Andrea Resta, Bénédicte Ealet, and Guy Le Lay Phys. Rev. Lett. 108, 155501 (2012)

Contribution of NCSR-D (7 person months):

Growth and in-situ characterization of Ge on Ag (111)

Brief Summary: NCSR-D continued the work on the Ge-deposited Ag(111) surfaces which was first reported in D2.1. Two different superstructures were observed- one of them being the “typical” ($\sqrt{3}\times\sqrt{3}$)R30°- in different coverage ranges. In addition, differences in the valence band features along the Γ M direction were also evident for the two surface reconstructions, whereas spectra recorded along the Γ K direction exhibit a bare Ag(111)-like behavior. Finally, a Ge-“decorated” Ag(111) template was examined as a possible substrate material for Si overgrowth. These additional data imply that there exists some interesting structures for further exploration but they cannot confirm at this stage the formation of germanene on Ag (111).

(a) Experimental details

Commercially purchased Ag(111) high-purity crystals were used as the substrate material. Before Ge deposition, Ar⁺ sputtering (1.5 KeV, 30 mins, P=5x10⁻⁵ mbar) and annealing (500 °C, 30mins) cycles were deployed in order to ensure clean, well-ordered Ag surfaces. Ge was evaporated from a Ta effusion cell heated at 1050 °C at an estimated deposition rate of 4x10⁻⁴ Å/s, while the substrate temperature was kept at RT. Various deposition times in the 35-150 mins range were used. Deposited samples were analyzed *in-situ* by RHEED, XPS, LEISS and UPS. For the combined Ag(111)/Ge/Si sample, a deposition time of 45 mins for both materials was used.

(b) LEISS monitoring of the Ge surface coverage

The coverage of the clean Ag(111) surface by the Ge overlayer was monitored by recording the LEIS spectra at an energy of 1 keV (Figure 1). Subsequently the integrated Ge/Ag intensity ratio was plotted as a function of the Ge deposition time (Figure 1, inset). It can be seen that at 80 mins Ge deposition time an abrupt change in the slope occurs, indicating the possible formation of 1 ML at this point.

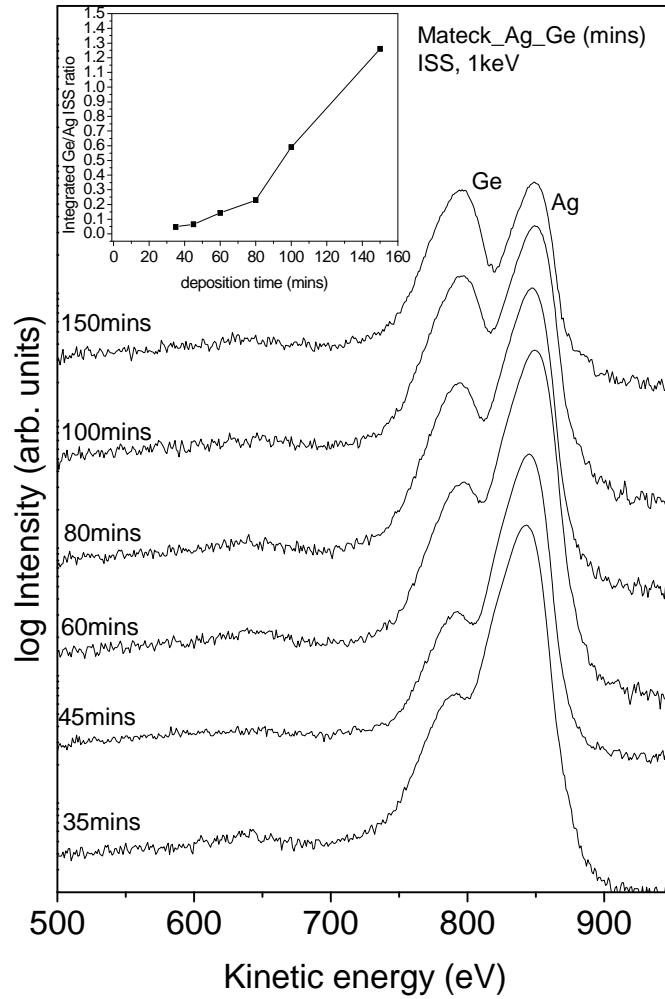


Figure 1: (a) LEISS spectra of the Ge-deposited Ag(111) samples for various Ge deposition times. The inset shows the integrated Ge/Ag intensity ratio indicating an 1 ML coverage at about 80 min dep. time.

In contrast to the case of Si/Ag (111) (see D2.1) where the coverage had a maximum around 70 min deposition, here, the coverage continues to increase after 80 min deposition indicating a different growth mechanism for the Ge/Ag (111) system.

(c) RHEED monitoring of the Ag(111)/Ge and Ag/Ge/Si MBE-deposited surfaces

The RHEED patterns recorded for the Ag(111)/Ge samples reveal the formation of two different surface reconstructions, depending on the Ge deposition time. As indicated in Figure 2,

for short Ge deposition (i.e 35-45 mins), a 3x1 RHEED pattern is observed compatible with the $(\sqrt{3}\times\sqrt{3})R30^\circ$ superstructure as revealed by LEED previously reported by Oughaddou et al [1,2].

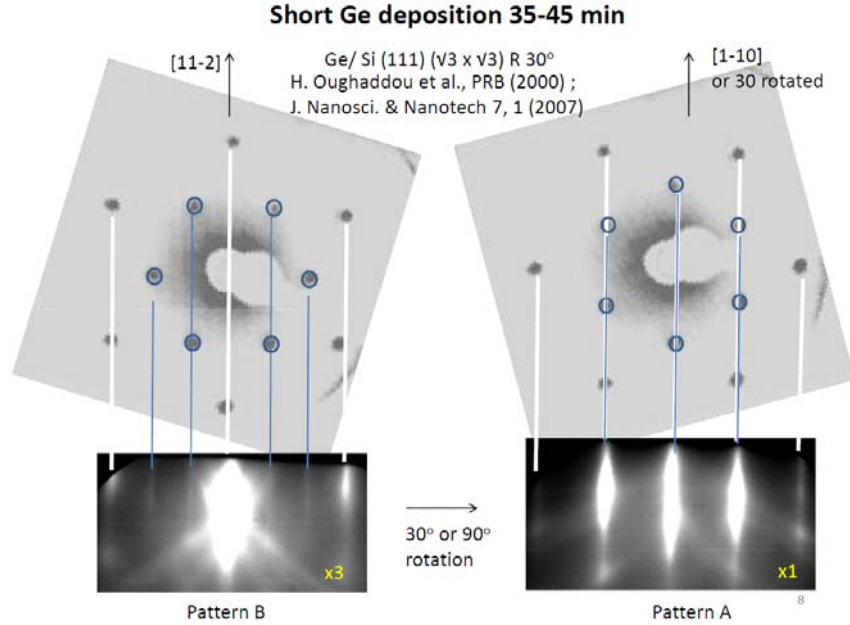


Figure 2: RHEED patterns obtained for short Ge deposition times (35-45 mins) on Ag(111). Pattern B is recorded along the [11-2] azimuth, whereas Pattern A along its perpendicular [1-10] azimuth. In the upper part of the figure LEED patterns of the $(\sqrt{3}\times\sqrt{3})R30^\circ$ are also shown for comparison

Moreover, for longer deposition times ((i.e. 80-150 mins) a more complicated RHEED pattern is recorded (Figure 3) which is compatible with the $\sqrt{3}\times 7$ LEED pattern and associated Ge tetramers as previously reported by Oughaddou et al [2]. At intermediate Ge deposition times (i.e. 60 mins), a mixed reconstruction pattern is observed [$(\sqrt{3}\times\sqrt{3})R30^\circ+\sqrt{3}\times 7$] (not shown here).

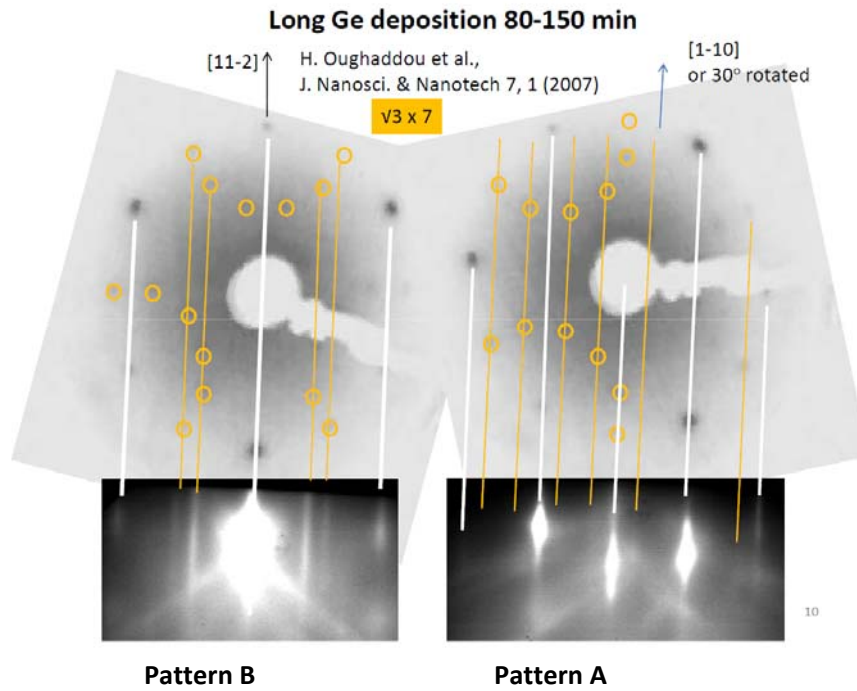


Figure 3: RHEED patterns obtained for long Ge deposition times (80-150 mins) on Ag(111). Pattern B is recorded along the [11-2] azimuth, whereas Pattern A along its perpendicular [1-10] azimuth. In the upper part of the figure LEED patterns of the $\sqrt{3} \times 7$ structure are also shown for comparison.

In a different experiment, we first deposited Ge on Ag(111) for about 45 min to produce the usual $(\sqrt{3} \times \sqrt{3})R30^\circ$ superstructure (3×1 in RHEED). Using this as a template we then deposited Si for 45 min to produce a Ag(111)/Ge/Si multilayer system. The RHEED patterns are shown in Fig. 4.

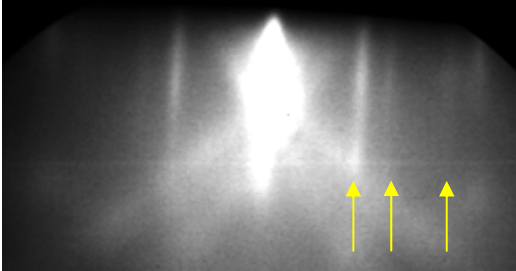
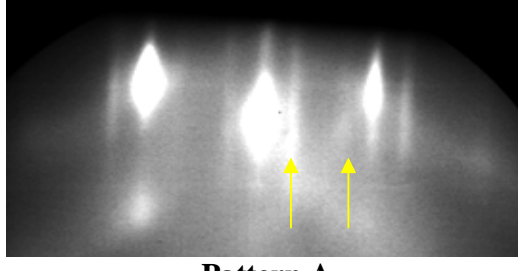
Sample	[11-2]	[1-10]
Ag_Ge45mins_Si45mins	 <p>Pattern B</p> <ul style="list-style-type: none"> • Similar to $\sqrt{3}\times 7$ pattern 	 <p>Pattern A</p> <ul style="list-style-type: none"> • Similar to $\sqrt{3}\times 7$ pattern • Or $\times 4$ structure, with missing middle streak

Figure 4: RHEED patterns obtained for the Ge(45mins)/Si(45mins) deposited sample on Ag(111). Pattern B is recorded along the [11-2] azimuth, whereas Pattern A along its perpendicular [1-10] azimuth.

Remarkably, in this case, the Si superstructure is different than the 4×4 pattern obtained when Si is directly deposited on Ag(111). The RHEED patterns in Fig. 4 indicate a superstructure which is very similar to that formed by Ge at long deposition times (Fig. 3), indicating that both Ge and Si form the same superstructure when they are deposited on an initially Ge-“decorated” Ag(111) template with the $(\sqrt{3}\times\sqrt{3})R30^\circ$ superstructure. Despite the fact that the [1-10] azimuthal RHEED pattern can be analysed with the help of a previously reported $\sqrt{3}\times 7$ structure [2], it is also possible that this pattern shows a $\times 4$ superstructure with the middle streak missing (forbidden diffraction streak), so the RHEED observations must be treated with care to avoid misinterpretation. Only a complete LEED measurement could resolve the puzzle.

(c) Valence band structure for the Ag(111)-Ge deposited surfaces

Although the main results along the $\square\square$ direction have already been reported in D2.1, here we describe some additional data in order to gain more insight about the influence of the Ge overlayer on the electronic band structure of Ag (111). The results are given in Fig. 5. The ARUPS data at two given polar angles are being plotted for various deposition times. On the left plot, a broad signal around 1 eV is present in clean Ag(111) and in high Ge coverage Ge/Ag(111) but it is totally absent in the low Ge coverage samples (35 and 45 min deposition) corresponding to samples with the $(\sqrt{3}\times\sqrt{3})R30^\circ$ dominant superstructure. On the other hand, in

the right plot, a sharp peak around 1 eV is present only for the low coverage (35 and 45 min deposition) samples with the characteristic $(\sqrt{3}\times\sqrt{3})R30^\circ$ superstructure, while it is absent for the bare Ag and the high Ge coverage samples. In general, from both plots in Fig. 5, it can be inferred that the Ge strongly modifies the Ag valence band structure near the M point only at low Ge coverage for which Ge forms the $(\sqrt{3}\times\sqrt{3})R30^\circ$ superstructure. At larger Ge coverage, the band structure looks very much the same as in bare Ag (111) as if the Ge has no influence on the Ag valence band near E_F . These findings are under further investigation, although at this stage, **it cannot** be said that these results constitute a signature for germanene formation.

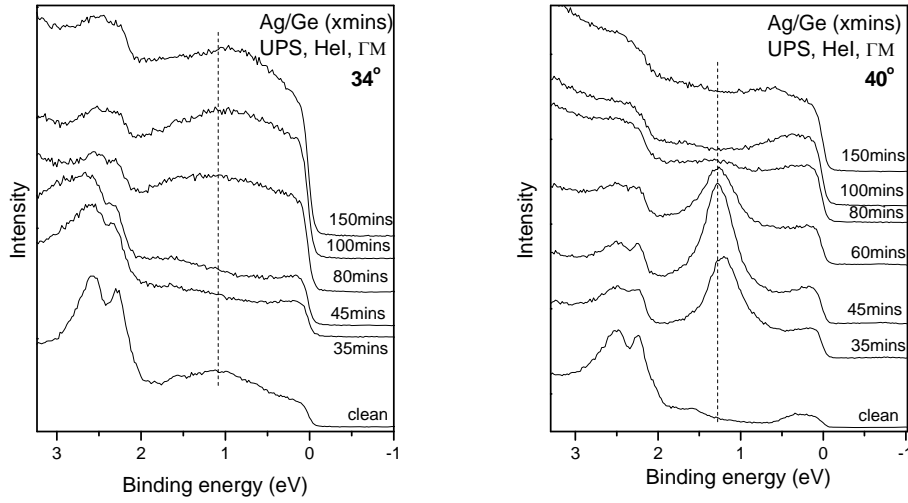


Figure 5: UPS spectra recorded at polar angle of 34° and 40° for various Ag/Ge-deposited samples. The intense feature at ~ 1 eV BE (right plot), is only present in the case of low Ge coverage, indicating a correlation to the $(\sqrt{3}\times\sqrt{3})R30^\circ$ superstructure.

Figure 6 presents the ARUPS data recorded for the clean and the 45 mins Ge-deposited Ag surfaces, along the ΓK direction. Upon Ge deposition, the weak dispersing band of the bare Ag surface only slightly modifies, in contrast with the spectra recorded along the ΓM direction (already presented in D2.1) where a big modification near the M point of Ag was observed after Ge deposition.

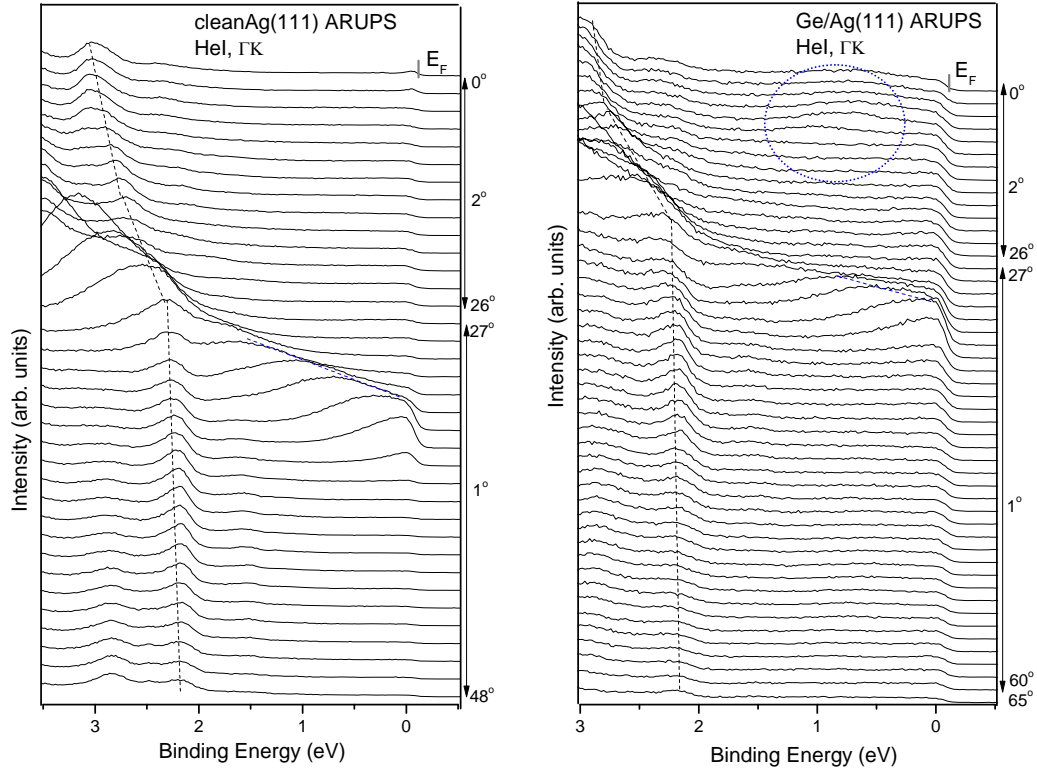


Figure 6: ARUPS spectra for clean and 45 min Ge deposited samples at different polar angles θ along the ΓK direction. The broken line circle marks the area at low polar angle (low k_{\parallel}) values at which a weak signal characteristic of Ge is present

Here, the only noticeable effect of the Ge overlayer is a small dispersive feature at small angles (see dashed circle line in Fig. 6) which was also observable in the ΓM spectra reported in D2.1.

In Figure 7, the ARUPS spectra along ΓK for the Ag/Ge/Si structure is presented. No big differences are obtained with respect to the case of Si directly deposited on Ag(111) with the 4x4 trigonal superstructure (D2.1). The wide dispersive signal is reminiscent of the Ag sp band which has been observed as the dominant feature in several other Si on Ag samples. In conclusion, although a new superstructure has been identified on the basis of RHEED data in Fig.4, the ARUPS data do not show any significantly different valence band structure and do not present any evidence toward a silicene structure on Ag/Ge template.

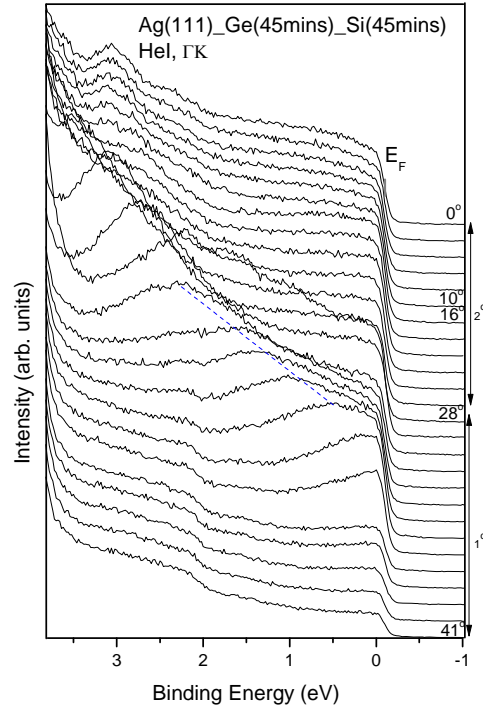


Figure 7: ARUPS spectra Ag/Ge/Si sample at different polar angles θ along the ΓK direction.

- [1] H. Oughaddou S. Sawaya, J. Goniakowski, B. Aufray, G. Le Lay, J. M. Gay, G. Treglia, J.P. Biberian, N. Barrett, C. Guillot, A. Mayne, and G. Dujardin, Phys. Rev. B 62, 16653 (2000)
- [2] H. Oughaddou, A. Mayne, B. Aufray, J.P. Biberian, G. Le Lay, B. Ealet, G. Dujardin, and A. Kara, J. Nanosci. & Nanotech 7, 1 (2007)

CNR-IMM (12 person months)

D3.1.1 B. In situ STM identification of the honeycomb structure of 2D-nanolattices of silicene, germane on metal substrates

CNR-IMM / *In situ STM-STs investigations of the local structural and electronic properties of differently buckled silicone phases*

Inspired by the identification of the silicene structure proposed by Vogt et al [1], an *in situ* characterization of the silicene structure as a function of the growth parameters (a), and of the local density of states (DOS) of the silicene layers epitaxially grown on Ag(111) substrates (b) has been performed by means of spatially resolved scanning tunneling microscopy (STM) and spectroscopy (STS), therein revealing non trivial local structural and electronic properties due to different kind of bonding distortion (e.g. buckling) and/or interaction with the substrate. In particular, it will be clarified that the observed silicene does not appear in a strictly graphene-like planar honeycomb arrangement but bond buckling imparts vertical distortions to the silicene surface structure which influence the STM and STS data.

(a) STM investigations of the silicene epitaxially grown on Ag(111) surfaces

Deposition of Si has been studied in the sub-monolayer regime as a function of the two relevant growth parameters, the substrate temperature T_s and the Si coverage θ for a fixed Si flux of (as calibrated by *in situ* quartz μ balance, *in situ* post-growth XPS probing of the Si 2*p* and Ag 4*s* lines, and *in situ* post-growth STM).

In this respect, Figure B1 shows a selection of STM topographies with increasing coverage (left-to-right) at $T_s \approx 250$ °C (Figure B1a,c,e). The presence of a Si layer has been ensured by *in situ* XPS probing of the Si 2*p* line (representatively reported for in Figure 1f for the morphology observed in Figure B1c) for each deposition experiment. The deposition of a Si layer with $\theta \approx 0.45$ ML (Figure B1a) involves the formation of 2D flat domains (see Figure B1b) - denoted as 2D-fl in the following - which apparently do not evidence any characteristic surface structure. The 2D flat region are tentatively interpreted as a lattice of Si atoms exactly placed in between the Ag surface atoms so as to constitute a perfectly unbuckled silicene arrangement as pictured in Figure B1b. Higher resolution imaging hardly performed over flat domains (an example is reported as inset in the inset of Figure B1a) evidences the presence of aligned dark centers. In addition, the magnification reported in Figure B1b evidences the presence of slightly bright protrusions (indicated with two cyan spots in the bottom panel of Figure B1b) at the center of each dark center, as schematized with the help of the overlapped lattice. This particular structure suggests a perfect match and alignment between the honeycomb Si and the underlying Ag lattice, as sketched in the bottom of Figure B1b. This picture would require a strong contraction (about the 23%) of the honeycomb structure compared with the simulated stable forms of silicene [2,3] with the consequence of a reduced Si-Si distance (≈ 0.17 nm) with respect to the predicted value of 0.22 nm, but the presence of Si atoms intercalated in between of Ag atoms is probably responsible of the experienced difficulty in recording clear atomically resolved STM images in correspondence of these flat domains because of a strong overlapping of the Ag and Si orbitals. Nonetheless, it is not clear at the moment whether the proposed disposition can be reasonably assigned to a true silicene

structure, due to the strongly contracted Si-Si distance. To this respect, STS measurements of the LDOS in the following are intended to reveal the electronic signature of this phase along with the other observed phases but further investigations, such as ARPES or Raman spectroscopy, are needed to recognize the presumed graphene-like arrangement.

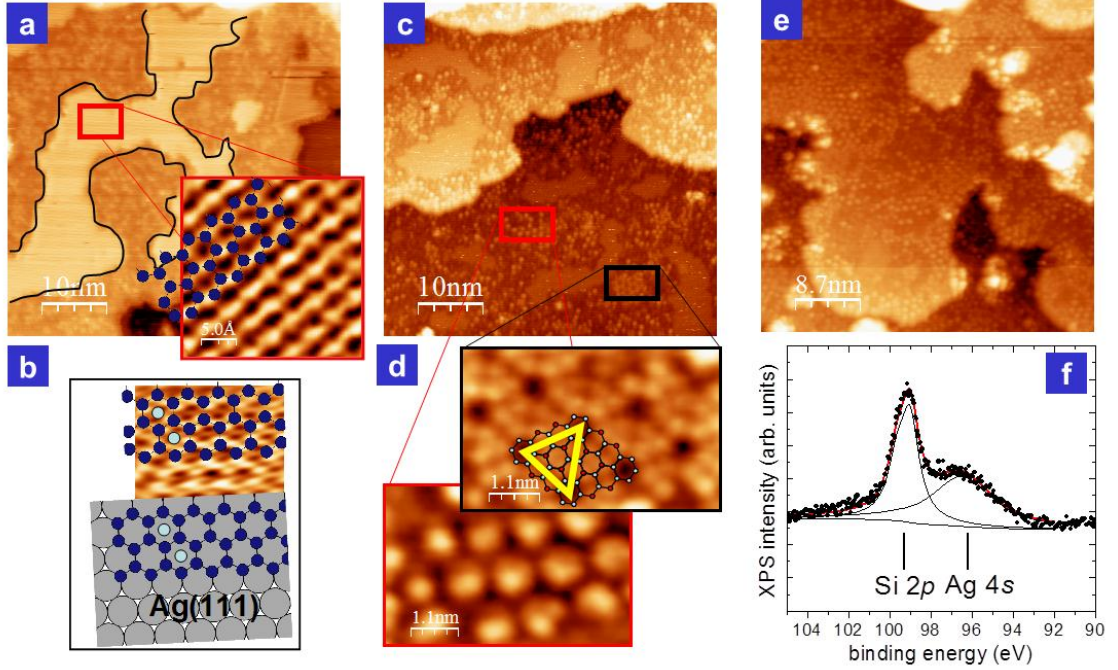


Figure B1 STM characterization of epitaxial Si on Ag(111) substrate temperature $T_s \approx 250$ °C. (a) STM image of a Si ad-layer with nominal thickness $\theta \approx 1.6$ Å ($V=-1.3$ V, $I=0.2$ nA); a high resolution STM magnification is shown as inset. (b) Filtered high resolution image of a 2D-fl domain ($V=-1.3$ V, $I=0.15$ nA) and a suggested hard sphere model. (c) Surface morphology after the deposition of a Si ad-layer with nominal thickness $\theta \approx 1.6$ Å ($V=-1.3$ V, $I=0.1$ nA). (d) High resolution images from a 4x4 domain (black contour) ($V=-1.5$ V, $I=0.4$ nA) and a 2D-dot domain (red contour) ($V=-1.5$ V, $I=0.4$ nA). (e) XPS spectrum of the Si 2p and the Ag 4s core level photoemission lines; the spectrum is fitted by convolving two pseudo-Voigt functions.

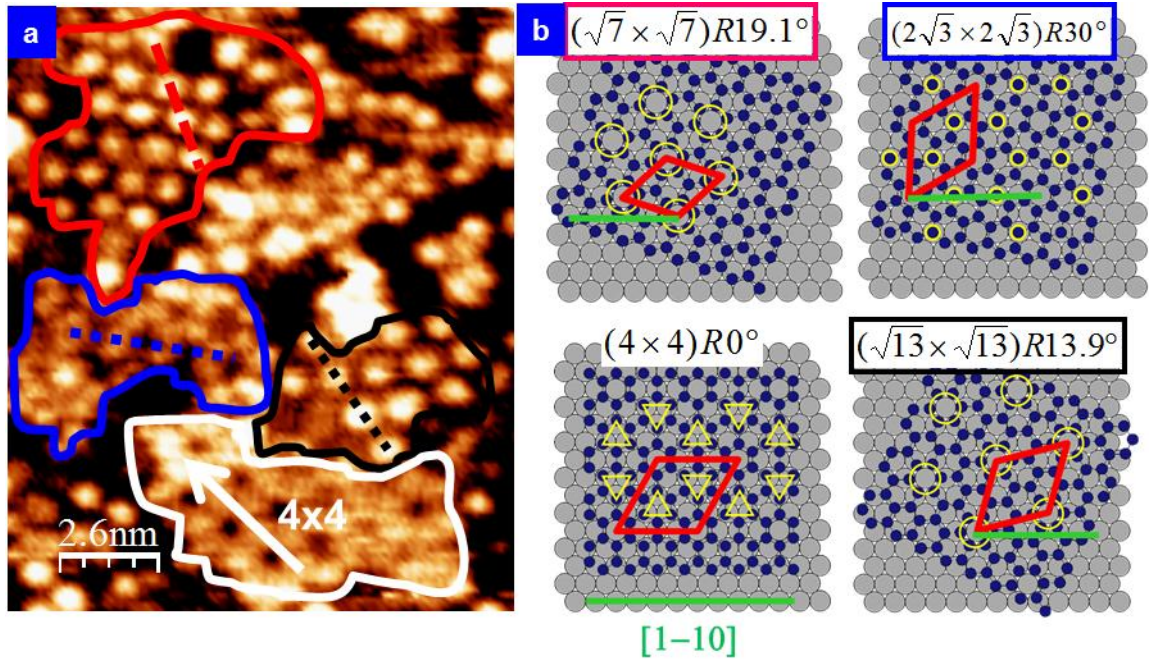


Figure B2 STM characterization of multi-orientated silicene domains on Ag(111). (a) Based on an equalized STM image, a pictorial view of individual Si domains which patch together to form a larger interconnected sheet. Each domain exhibits a characteristic orientation with respect to the Ag substrate; the arrow indicates the $[1-10]$ direction of the Ag(111) surface, while dotted guidelines (red, blue and black) distinguish the different preferential orientations. (b) Sequence of hard sphere models which simulate the superposition of oriented honeycomb silicene lattices (blue spots, yellow contours mark the protruding Si atoms which give rise to the registered STM topography) on the Ag(111) surface (grey spots) which correspond to the differently oriented domains in panel (a).

With increasing the nominal coverage ($\theta \approx 0.65$ ML, Figure B1b), 2D flat domains and small silicon domains with complex surface structures coexist on the silver surface. Increasing further the nominal coverage ($\theta \approx 0.90$ ML, Figure B1c) the previously observed structured domains enlarge and tend to fully cover the Ag surface. Concomitantly we can notice the complete suppression of flat domains (2D-fl). The structured domains exhibit non-trivial surface morphologies which can be distinguished in two characteristic arrangements either in Figures B1c and B1e: a (4×4) superstructure (see the magnification in the black frame in Figure B1d) and periodic patterns made up of hexagonally packed dots (2D-dots, see the magnification in the red frame in Figure B1d). As recently demonstrated [1,4], the STM detection of (4×4) domains has proven to be an indirect evidence of the presence of a buckled form of silicene [1,4]. As for the dotty pattern, a comparative analysis is facilitated by the presence of small single layer domains that patch together like a quilt to form larger sheets, as shown in Figure B2a. Single STM images can access all the characteristic morphologies, thus avoiding ambiguities which may result from tip artifacts or thermal drift. In particular, the latter effect is quite important to notice because it may jeopardize a good

estimation of relative orientations of single domains. Indeed, the STM image in Figure B2b evidences the local presence of patterned domains (2D-dots) with different periodicities and orientations. The alignments of the various domains can be easily compared with the [1-10] direction of the Ag(111) surface (black arrow in Figure B2b) which pointedly corresponds to the orientation of the (4x4) domain (white contour in Figure B2a), i.e. there is no misalignment between the Ag(111) surface lattice and the (4x4) super structure of the silicene layer. Two dominant patterns can be distinguished with periodicities $\lambda_{D1} = 1\text{ nm}$ (black contour and dotted lines) and $\lambda_{D2} = 0.8\text{ nm}$ (red contour and dotted lines) with an accuracy of 0.5 nm. Their misalignment with respect to the [1-10] direction of the Ag(111) surface is respectively 13° and 20° (with an accuracy of around $\pm 2^\circ$). In addition, a more complex structure (blue contour and dotted lines) can be also observed which is made up of hexagonal crowns of Si atoms with periodicity $\lambda_H = 1\text{ nm}$ and misalignment of 30° . The observed dotty pattern along with (4x4) silicene structure are interpreted to stem from differently bonding distortion of the same hexagonal silicene arrangement as elucidated in the hard sphere schemes in Figure B2b for each kind of domain in Figure B2a. In particular, the observed characteristic patterns can be respectively identified with the $(4 \times 4)R0^\circ$, $(\sqrt{13} \times \sqrt{13})R13.9^\circ$, $(\sqrt{7} \times \sqrt{7})R19.1^\circ$, and $(2\sqrt{3} \times 2\sqrt{3})R30^\circ$ superstructures (the corresponding unit cells are represented in red in Figure B2b). The large bright spots which constitute the observed dot structures (2D-dots) result from the tip-convolution of adjacent Si atoms which are placed “on-top” with respect to the underlying Ag atoms, as happens for the observed $(\sqrt{13} \times \sqrt{13})R13.9^\circ$ and the $(\sqrt{7} \times \sqrt{7})R19.1^\circ$ arrangements.

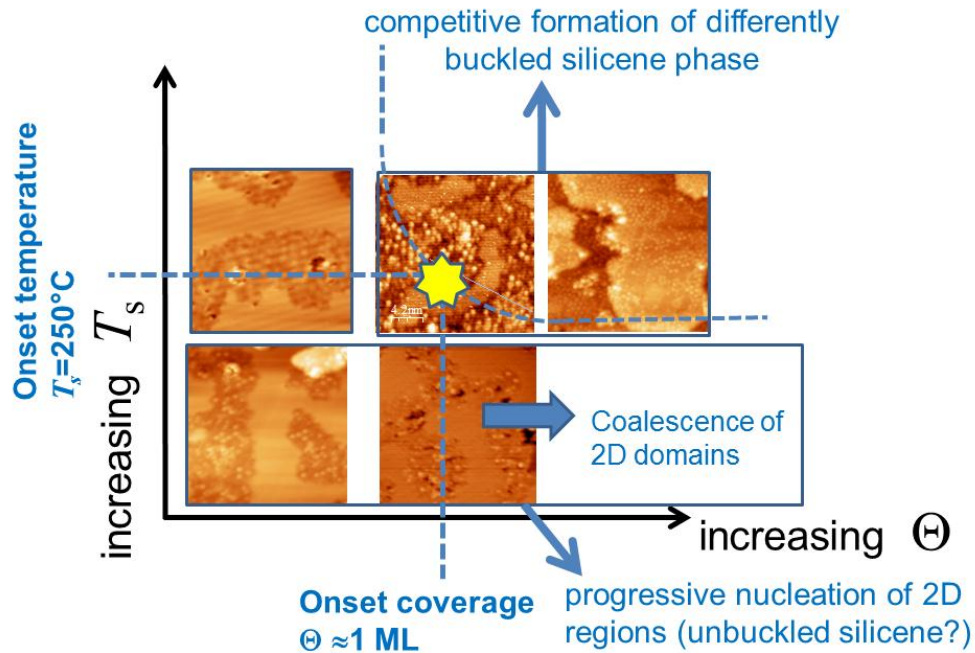


Figure B3 Phenomenological surface phase diagram for the Si epitaxy on Ag(111) with the growth temperature T_s and the film coverage Θ as thermodynamical parameters (STM topographies are taken from the analysis presented in Figure 1). The yellow star at mid-diagram identifies the onset values of T_s and Θ for the buckled silicene phases to form.

Similar deposition experiments have been reproduced at lower substrate temperatures T_s for equivalent coverage values of the Si ad-layers (supporting information). It follows that, when $T_s < 240$ °C, no structural transitions from flat domains to structured domains can be observed. To rationalize the Si structures observed in different growth conditions, a phenomenological diagram of the surface structural phases is illustrated in Figure B3 taking T_s and θ as thermodynamical driving quantities. These preliminary observations suggest that silicon ad-layers undergo 2D structural transitions in the monolayer thickness regime. These mechanisms are thermally activated and critically depend on the substrate temperature and on the nominal thickness of Si as trade-off parameters for the transitions from one phase to another one.

(b) STS investigations of the silicene epitaxially grown on Ag(111) surfaces

In the effort to discriminate the electronic character of the silicene phases, STS investigations of the local density of states (LDOS) have been performed on the various 2D morphologies observed in the silicon ad-layers upon taking the STS curves of the freshly recovered Ag(111) surface and a separately prepared Si(111) surface as references. This effort provides a deeper insight into the local spectroscopy of silicene. $I(V)$ and dI/dV curves (Figure B4) have been collected in spectroscopy mode over the clean Ag(111) surface and Si(111) surface as references, and - after Si deposition - over Si covered zones which exhibit the characteristic morphologies shown in Figure B1, i.e. flat (2D-fl) or structured domains (e.g. (4x4), and other dotty patterns). In particular the STS characterization of structured domains has been limited here to the characteristic surface patterns corresponding to the (4x4) and $(\sqrt{13} \times \sqrt{13})$ reconstructions (see Figure B1e), and to the 2D flat domains (see Figure B1a), as discussed above (see Figure B2). In Figure B4a the $I(V)$ and dI/dV curves of the Si(111) and Ag(111) surfaces respectively evidences an expected well-defined gap-like feature and a characteristic quasi-linear trend for the Ag(111) surface indicative of the continuum of states typical of metals. When the Si wetting layer is STS-probed, the $I(V)$ plot exhibits a significantly different profile compared with the one recorded on the freshly cleaned Ag(111) surface irrespectively of the measured morphology, (4x4), $(\sqrt{13} \times \sqrt{13})$, and 2D-flat domains. Indeed, a strong reduction of the curve slope can be identified while spanning the tip voltage V_{tip} from -0.2 V to +0.6 V. This behavior can be associated with a relative reduction of the LDOS around the Fermi level, as evidenced by the dI/dV tunneling spectrum shown in Figure B4b: a plateau-like feature corresponds to the just identified low LDOS region which is comprised between two lateral branches. It is important to notice that no characteristic feature can be recognized which could be attributed to the Ag substrate (Figure B3b). A similar behavior is roughly reproduced when probing the $I(V)$ of the three probe Si domains. However deviations in the STS profiles of the three morphologies occurs when accounting for the STS profile close to the Fermi energy (i.e. 0 bias) which can be related either to different atomic arrangement or to a role of the buckling in the LDOS. It is worth to mention that the reported curves are averaged on a large number of curves taken in different position throughout the corresponding domain.

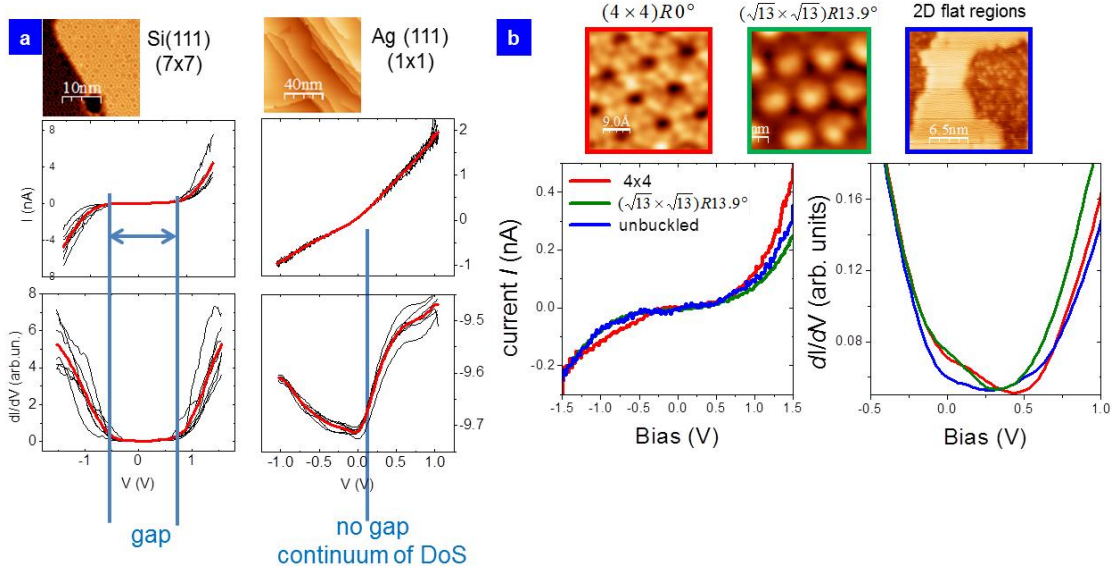


Figure B4 (a) $I(V)$ and dI/dV curves taken on in situ recovered (7x7) reconstructed Si(111) (left) and (1x1) Ag(111) (right) surfaces (the corresponding topographies are reported on the top side). The gap like features in the Si(111) related curves and the continuum of states in the Ag(111) related curves are emphasized. (b) $I(V)$ and dI/dV curves taken for the (4x4) phase (see the topography in the red frame and the corresponding red curves), the $(\sqrt{13} \times \sqrt{13})$ phase (see the topography in the green red frame and the corresponding green curves), and 2D-flat domain (see the topography in the blue frame and the corresponding blue curves).

Two sequences of individual STS spectra are reported which were obtained by sampling different positions of (4x4) domains (Figure B5a) and $(\sqrt{13} \times \sqrt{13})$ domains (Figure B5b). A representative morphology is shown in Figure 5c, where the sampled domain areas are respectively indicated in red and grey contours. In both morphologies, the STS curves appears to follow a twofold fashion which is not trivially related to stochastic fluctuations. Indeed, both the sequences in Figure B5a and B5b evidence the presence of two characteristic families of STS curves which have been distinguished in blue and green traces respectively. The green curves exhibit a zero-gap fashion centered on a minimum which is located at a tip voltage $V_A \approx +0.25$ V. The blue curves present two characteristic “elbows” which are symmetrically placed around V_A at -0.2 V and $+0.6$ V (vertical dotted lines). The bimodal distribution of STS curves demonstrates that the nature of the spectral fluctuations is not stochastic but is more intriguingly related to a position dependent DOS of the highly-buckled silicene. This observation suggests that the interactions between the silicene lattice and the Ag(111) surface might be responsible for local alterations of the tunneling conductance which arise from the structural transition from flat domains to structured domains (highly-buckled). It should be noticed that modifications of the electronic structure in epitaxial graphene (e.g. band gap opening) were ascribed to substrate induced breaking of the sublattice symmetries [5]. Similarly, a symmetry breaking can be provoked by the different reconstructions observed in the silicene domains [5]. It is worth noting that the two families of STS curves obtained by

sampling $(\sqrt{13} \times \sqrt{13})$ domains evidence some relevant differences with respect to those obtained from (4×4) domains, in particular for positive voltages beyond the plateau region. This effect suggests that the orientation of silicene domains on the Ag(111) has an impact in the LDOS distribution, thus also hinting at an orientation dependent modulation of the local interactions between the silicene domains and the Ag substrate.

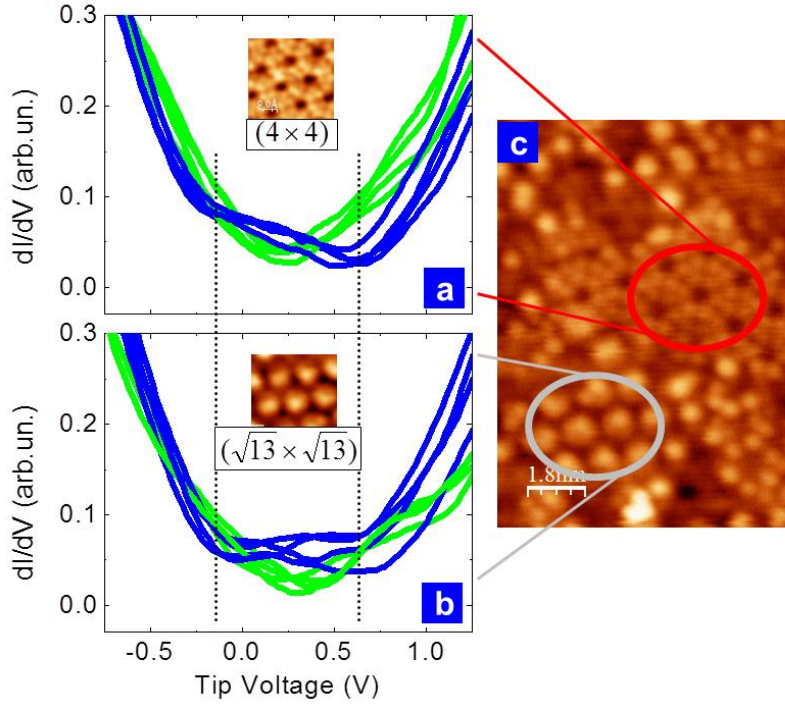


Figure B5 Spatial modulation of STS spectra. (a) Individual dI/dV spectra obtained by sampling different regions over a (4×4) silicene domain; (b) A similar STS characterization from a dotted domain $(\sqrt{13} \times \sqrt{13})$; two families of curves can be distinguished (green and blue traces). (c) Representative STM topograohy where the STS-sampled areas are indicated through the red (2D- 4×4) and grey contours (2D-dots).

List of references

1. Vogt, P.; De Padova, P.; Quaresima, C.; Avila, J.; Frantzeskakis, E.; Asensio, M. C.; Resta, A.; Ealet, B.; Le Lay, G. *Phys. Rev. Lett.* 2012, 108, 155501.
2. Cahangirov, S.; Topsakal, M.; Akturk, E.; Sahin, H.; Ciraci, S. *Phys. Rev. Lett.* 2009, 102, 236804.
3. Houssa, M.; Pourtois, G.; Afanasev, V. V.; Stesmans, A. *Appl. Phys. Lett.* 2010, 97, 112106.
4. Lin, C.-L.; Arafune, R.; Kawahara, K.; Tsukahara, N.; Minamitani, E.; Kim, Y.; Takagi, N.; Kawai, M. *Appl. Phys. Express* 2012, 5, 045802.
5. Zhou, S. Y.; Gweon, G. H.; Fedorov, A. V.; First, P. N.; De Heer, W. A.; Lee, D. H.; Guinea, F.; Castro Neto, A. H.; Lanzara, A. *Nat. Mater.* 2007, 6, 770.

Publication

Exploring the new physics of two-dimensional silicon: Local characterization of silicene films on Ag(111)

Daniele Chiappe, Carlo Grazianetti,, Grazia Tallarida, Marco Fanciulli, Alessandro Molle
Advanced materials, in press

Conclusion

The results obtained in a 12 month period by CNRS/Aix-Marseille University, NCSR-D and CNR-IMM demonstrate that both structural and electronic properties of the 2D Si/Ge ad-layers formed on Ag(111) and other (111) surfaces are quite complicate, even if the (4x4) 2D Si ad-layer on Ag(111) establishes for the first time the real synthesis of 2-dimensional silicene sheets.

Indeed, this demands more characterizations and, especially, further exploration for Ge before the formation of germanene can be safely confirmed.